Stochastic resetting and first arrival subjected to Gaussian noise and Poisson white noise

Koushik Goswami and Rajarshi Chakrabarti [*]

Department of Chemistry, Indian Institute of Technology Bombay, Mumbai, Powai 400076, India

We study the dynamics of an overdamped Brownian particle subjected to Poissonian stochastic resetting in a nonthermal bath, characterized by a Poisson white noise and a Gaussian noise. Applying the renewal theory we find an exact analytical expression for the spatial distribution at the steady state. Unlike the single exponential distribution as observed in the case of a purely thermal bath, the distribution is double exponential. Relaxation of the transient spatial distributions to the stationary one, for the limiting cases of Poissonian rate, is investigated carefully. In addition, we study the first-arrival properties of the system in the presence of a delta-function sink with strength κ, where $\kappa = 0$ and $\kappa = \infty$ correspond to fully nonreactive and fully reactive sinks, respectively. We explore the effect of two competitive mechanisms: the diffusive spread in the presence of two noises and the increase in probability density around the initial position due to stochastic resetting. We show that there exists an optimal resetting rate, which minimizes the mean first-arrival time (MFAT) to the sink for a given value of the sink strength. We also explore the effect of the strength of the Poissonian noise on MFAT, in addition to sink strength. Our formalism generalizes the diffusion-limited reaction under resetting in a nonequilibrium bath and provides an efficient search strategy for a reactant to find a target site, relevant in a range of biophysical processes.

I. INTRODUCTION

In the mesoscopic world, diffusion refers to the random motion of Brownian particles in a fluid at thermal equilibrium. In this case, the detailed balance as well as congruent features such as the fluctuation-dissipation theorem (FDT) and zero heat flux are maintained [1]. In other words, diffusion is a passive process as it takes place in thermal equilibrium. In recent years, there has been growing interest in studies of active particles, which are self-driven due to the consumption of energy from their surroundings and therefore away from equilibrium [2–4]. Models such as active Brownian particles (ABPs) and run-and-tumble particles (RTPs) have been used extensively for their dynamical descriptions incorporating the persistence in their motion [5–7]. Evidently, when a passive molecule such as colloid or polymer is immersed in a bath containing active particles, the molecule behaves differently from a thermal (or equilibrium) bath [8–10]. Apart from the thermal noise, it experiences additional nonequilibrium fluctuations (active noise) which drives the system away from equilibrium [10–17]. The peculiarities of its dynamics are often encoded in its distribution function which, in some cases, is found to be non-Gaussian in nature [18–20]. For instance, the motion of a tracer particle inside the cytoskeleton network has been found to be non-Gaussian consisting of two parts: the Gauss-like central region followed by an exponential tail [18]. Such tail occurs due to the athermal noise stemming from the power stroke generated by motor proteins, and the noise can be conceived as the Poisson one. In practice, the

Poissonian noise has been widely used as an effective model for non-Gaussianity in biological systems, for instance, to explain membrane undulations [21,22], neuron dynamics [23], swelling of a polymer [24], etc. If the system does not have any memory effect, or roughly speaking, the dynamics is Fickian, not necessarily, one should invoke a finite correlation time in the noise statistics to describe it. Sometimes memoryless fluctuations can render an out-of-equilibrium state [15,17,25–28]. For this matter, the Poissonian shot noise is an ideal choice for characterization of an athermal bath to study Markovian, non-Gaussian dynamics [9,29]. Note that such noise has been previously employed for modeling several physical cases such as ATP hydrolysis in the context of movement of motor proteins [30], nonperiodic oscillatory distortion of a lipid interface coupled with actomyosin [31], and dynamics of a granular rotor in an environment containing low-density granular gases [26,32].

Search processes are very much intertwined with diffusion for small systems, particularly ones involved in diffusion-limited reactions. For example, during gene expression, a protein molecule (transcription factor) searches for a promoter site on the DNA chain to initiate transcription. Along with others, two main routes it adopts to find the target are three-dimensional excursions in the surroundings and one-dimensional diffusive search (sliding) along the DNA track [33–35]. A major goal in investigating such processes is to find a strategy for which the rate gets minimized. Along these lines, a lot of attention has rightfully been paid these days to the stochastic resetting, a mechanism for which a system undergoing a stochastic process is reset back at random times to a prescribed position and restarts the process all over again [36]. Two key features of diffusion processes with resetting

*rajarshi@chem.iitb.ac.in

are that (i) the system always achieves a nontrivial nonequilibrium steady state, and (ii) in the presence of a target, there exists an optimal rate for which the search time is finite and minimum [37,38]. No wonder the occurrence of such intriguing characteristics triggers exploring its different variants, namely, resetting with several processes such as continuous-time random walks [39], fractional Brownian motions [40], Lévy flights [41], underdamped diffusion [42], velocity-jump processes [43], and others [44,45]. Furthermore, the effect of various confining potentials [46–48] and diffusivities [49] on the resetting mechanism has been investigated thoroughly over the past few years.

The majority of the studies on resetting mentioned above have been carried out for diffusive systems in the thermal bath. Recently, a number of groups have explored the possibility of incorporating the activity in the resetting mechanism [50–53]. A charged ABP subjected to a spatially nonhomogeneous magnetic field has been found to have a nonmonotonic density profile and a higher mean first-passage time compared to its passive counterpart [54]. Further developments have witnessed implications of stochastic resetting in the dynamics of RTPs which serves as the standard model for bacterial motion [51,53]. However, to the best of our knowledge, very little is known about the role of nonthermal fluctuations on a passive particle under a resetting mechanism. In this paper, our interest is to fill the existing gap in the literature, and try to provide a comprehensive study on the dynamics and first-passage properties of an activity-driven stochastic resetting process. To do so, here we consider a situation where a passive Brownian particle is diffusing in a nonthermal bath characterized by the Poissonian white noise. The particle is brought back randomly at a constant rate r to its initial position x_0, from where it restarts its journey following the underlying stochastic equation. Note that in our model, the epochs at which the particle returns to x_0 are drawn from a Poissonian distribution; that is to say, the waiting time distribution is given by $\psi_w(t) = re^{-rt}$. However, it may be possible to generalize the resetting mechanism by considering a generic form of $\psi_w(t)$; e.g., see Ref. [55]. In Sec. II we illustrate the effect of resetting on dynamical behaviors of the particle diffusing in an unbounded domain. At large times the particle relaxes to a stationary state, and the relaxation mechanisms for two limiting cases are discussed in Sec. III. Further we investigate the first-arrival properties of the system in the presence of a sink (or target) at some position x_S. When the particle meets the target, either it binds to the target instantaneously, i.e., it gets fully absorbed at $x = x_S$, or it may not identify the target with certainty, which is referred to as the partial absorption [56]. One common interest in such study is to find the rate and efficiency of the process. The efficiency is generally determined by the time it takes on average to reach the sink for the first time, which is called the mean first-arrival time (MFAT), and the distribution of MFAT known as the first-arrival time density (FATD) is a measure of the instantaneous rate. By finding those quantities, we demonstrate how first-arrival properties depend on the interplay between activity and resetting mechanism, as discussed in Sec. IV. It should be noted here that our theoretical model can be realized experimentally by mimicking the recent experimentation on the stochastic resetting [57] to corroborate the results. Finally, the summary of our findings is given in Sec. V.

II. STOCHASTIC RESETTING IN A FREE SPACE

Suppose a Brownian particle is moving in a free space in the nonthermal bath. It is subjected to the thermal noise $\eta_T(t)$ and an athermal noise $\xi_A(t)$. $\eta_T(t)$ is usually given by the symmetric, delta-correlated Gaussian noise which obeys the fluctuation-dissipation theorem (FDT): $\langle \eta_T(t_1)\eta_T(t_2)\rangle = 2D_T\delta(t_1 - t_2)$, where D_T is the diffusivity of the particle in the thermal bath. On the other hand, the noise $\xi_A(t)$ violates the FDT and so the bath can no longer be described by the equilibrium properties. Here we do not take into account the memory effect, and so $\xi_A(t)$ is taken as the Poissonian white noise. It can be realized as a sequence of delta pulses occurring at random times over a time interval $[0, t]$, viz., $\xi_A(t) = \sum_i a_i\delta(t - t_i)$. The occurrence of pulses follows the Poisson statistics with a Poisson rate μ, and the jump length associated with ith pulse denoted by a_i is drawn from the Laplace distribution of the form $\mathcal{P}(a) = \frac{1}{2a_0}e^{-\frac{|a|}{a_0}}$, where a_0 is the average jump length. It is easy to see that $\langle \xi_A(t)\rangle = 0$, and $\langle \xi_A(t)\xi_A(t')\rangle = 2D_A\delta(t - t')$, where the diffusivity due to the nonthermal noise is given by $D_A = \mu a_0^2$ [9].

Let us consider that the particle is initially at position x_0, and the probability density at position x after time t is $P_0(x, t)$. The density, or the propagator $P_0(x, t|x_0)$, evolves according to the following Kolmogorov-Feller equation [28,58]:

$$\frac{\partial}{\partial t}P_0(x, t) = D_T\frac{\partial^2}{\partial x^2}P_0(x, t) + D_A\frac{\frac{\partial^2}{\partial x^2}}{1 - a_0^2\frac{\partial^2}{\partial x^2}}P_0(x, t). \quad (1)$$

For an alternative derivation of the above equation, see Appendix A. In Eq. (1), the first term on the right-hand side (RHS) is given by a second-order derivative which describes the normal diffusion. In contrast to this, the final term contains a nonlocal differential operator which corresponds to the Poissonian noise. If one consider the limit $a_0 \to 0$ and $\mu \to \infty$ in such a way that D_A remains constant, the nonlocal property vanishes so that one recovers the normal diffusion case [59]. In general, an exact analytical solution of Eq. (1) is difficult to obtain. However, it can be treated analytically using the Fourier transform, defined as $\tilde{P}_0(p, t) = \frac{1}{2\pi}\int dx\, e^{-ipx}P_0(x, t)$. On doing the transform, Eq. (1) becomes

$$\tilde{P}_0(p, t) = e^{-D_Tp^2t - D_At\frac{p^2}{1 + a_0^2p^2}}. \quad (2)$$

With this result, one can find several limiting cases for the spatial density. For more details, the reader is referred to Ref. [8].

We now address the resetting problem for the above stochastic process. Here we consider the Poissonian resetting protocol; i.e., the waiting times between two successive resetting events follow the exponential distribution with rate r. Also let us assume that the particle is reset to a resetting position which, for simplicity, is the same as the initial position x_0. For this case, the probability distribution function (PDF),

denoted by $P_r(x, t)$, satisfies the equation

$$\frac{\partial}{\partial t} P_r(x, t) = D_T \frac{\partial^2}{\partial x^2} P_r(x, t) + D_A \frac{\frac{\partial^2}{\partial x^2}}{1 - a_0^2 \frac{\partial^2}{\partial x^2}} P_r(x, t) - r P_r(x, t) + r \delta(x - x_0). \tag{3}$$

The last two terms account for the loss and gain of probabilities due to resetting, respectively. Taking the Fourier transform of Eq. (3), one obtains

$$\frac{\partial}{\partial t} \tilde{P}_r(p, t) = -D_T p^2 \tilde{P}_r(p, t) - D_A \frac{p^2}{1 + a_0^2 p^2} \tilde{P}_r(p, t) - r \tilde{P}_r(p, t) + r e^{-ipx_0}. \tag{4}$$

Without loss of any generality, here we take $x_0 = 0$, which makes the initial condition to be $P_r(x, 0) = \delta(x)$. After performing simple mathematical steps and rearranging the terms as shown in Appendix B, we obtain

$$\tilde{P}_r(p, t) = e^{-rt} \tilde{P}_0(p, t) + r \int_0^t dt' \, e^{-rt'} \tilde{P}_0(p, t'). \tag{5}$$

Upon doing the inverse Fourier transformation of the above, we have

$$P_r(x, t) = e^{-rt} P_0(x, t) + r \int_0^t dt' \, e^{-rt'} P_0(x, t'), \tag{6}$$

where $P_0(x, t)$ is the solution of Eq. (1), and it can be expressed as the inverse Fourier transform of Eq. (2), i.e., $P_0(x, t) = \int \frac{dp}{2\pi} e^{-ipx} e^{-D_T p^2 t - D_A t \frac{p^2}{1 + a_0^2 p^2}}$. One can easily recognize Eq. (6) as the last renewal equation for this process.

Now our motive is to obtain the density $P_r(x, t)$. For that, we go back to Eq. (5), and writing the expression for $\tilde{P}_0(p, t)$ explicitly with the aid of Eq. (2), we have

$$\tilde{P}_r(p, t) = e^{-rt} e^{-(D_T t p^2 + D_A t \frac{p^2}{1 + a_0^2 p^2})} + r \int_0^t dt' \, e^{-rt'} e^{-(D_T t' p^2 + D_A t' \frac{p^2}{1 + a_0^2 p^2})}. \tag{7}$$

In the final term, the integration over time can be easily done, and it yields

$$\tilde{P}_r(p, t) = e^{-rt} e^{-(D_T t p^2 + D_A t \frac{p^2}{1 + a_0^2 p^2})} + \frac{r(1 + a_0^2 p^2)\left[1 - e^{-rt} e^{-(D_T t p^2 + D_A t \frac{p^2}{1 + a_0^2 p^2})}\right]}{D_T a_0^2 p^4 + (D_A + D_T + a_0^2 r) p^2 + r}. \tag{8}$$

Further rearranging the terms, we arrive at an analytically tractable form as

$$\tilde{P}_r(p, t) = e^{-rt} e^{-(D_T t p^2 + D_A t \frac{p^2}{1 + a_0^2 p^2})} + \frac{r}{D_T}\left[1 - e^{-rt} e^{-(D_T t p^2 + D_A t \frac{p^2}{1 + a_0^2 p^2})}\right]$$
$$\times \left[\left(\frac{\alpha_3(r) - \alpha_1(r)}{\alpha_2(r) - \alpha_1(r)}\right) \frac{1}{p^2 + \alpha_1(r)} + \left(\frac{\alpha_2(r) - \alpha_3(r)}{\alpha_2(r) - \alpha_1(r)}\right) \frac{1}{p^2 + \alpha_2(r)}\right], \tag{9}$$

where $\alpha_3(r) \equiv \alpha_3 = \frac{1}{a_0^2}$, $\alpha_2(r) + \alpha_1(r) = \frac{D_A}{D_T} \frac{1}{a_0^2} + \frac{1}{a_0^2} + \frac{r}{D_T}$, $\alpha_1(r)\alpha_2(r) = \frac{r}{D_T} \frac{1}{a_0^2}$, which implies

$$\alpha_2(r) = \frac{1}{2a_0^2}\left[\frac{D_A}{D_T} + 1 + \frac{a_0^2 r}{D_T}\right] + \frac{1}{2a_0^2}\sqrt{\left[\frac{D_A}{D_T} + 1 + \frac{a_0^2 r}{D_T}\right]^2 - \frac{4a_0^2 r}{D_T}},$$

$$\alpha_1(r) = \frac{1}{2a_0^2}\left[\frac{D_A}{D_T} + 1 + \frac{a_0^2 r}{D_T}\right] - \frac{1}{2a_0^2}\sqrt{\left[\frac{D_A}{D_T} + 1 + \frac{a_0^2 r}{D_T}\right]^2 - \frac{4a_0^2 r}{D_T}}.$$

Now we can perform the inverse Fourier transform of Eq. (9), and it reads

$$P_r(x, t) = e^{-rt} P_0(x, t) + \frac{r}{D_T}\left[\left(\frac{\alpha_3(r) - \alpha_1(r)}{\alpha_2(r) - \alpha_1(r)}\right) \frac{e^{-\sqrt{\alpha_1(r)}|x|}}{2\sqrt{\alpha_1(r)}} + \left(\frac{\alpha_2(r) - \alpha_3(r)}{\alpha_2(r) - \alpha_1(r)}\right) \frac{e^{-\sqrt{\alpha_2(r)}|x|}}{2\sqrt{\alpha_2(r)}}\right]$$
$$- \frac{r e^{-rt}}{D_T} \int dx' \left[\left(\frac{\alpha_3(r) - \alpha_1(r)}{\alpha_2(r) - \alpha_1(r)}\right) \frac{e^{-\sqrt{\alpha_1(r)}|x'|}}{2\sqrt{\alpha_1(r)}} + \left(\frac{\alpha_2(r) - \alpha_3(r)}{\alpha_2(r) - \alpha_1(r)}\right) \frac{e^{-\sqrt{\alpha_2(r)}|x'|}}{2\sqrt{\alpha_2(r)}}\right] P_0(x - x', t). \tag{10}$$

The moment of the displacement can be calculated from the Fourier transform (9), using the relation, $\langle x^n(t) \rangle = (-i)^n \frac{\partial^n \tilde{P}_r(p, t)}{\partial p^n}\big|_{p=0}$. Since the process is symmetric in space, all odd moments are zero. The second moment or the mean square displacement (MSD) is computed as

$$\langle x^2(t) \rangle = \frac{2}{r}(D_A + D_T)(1 - e^{-rt}). \tag{11}$$
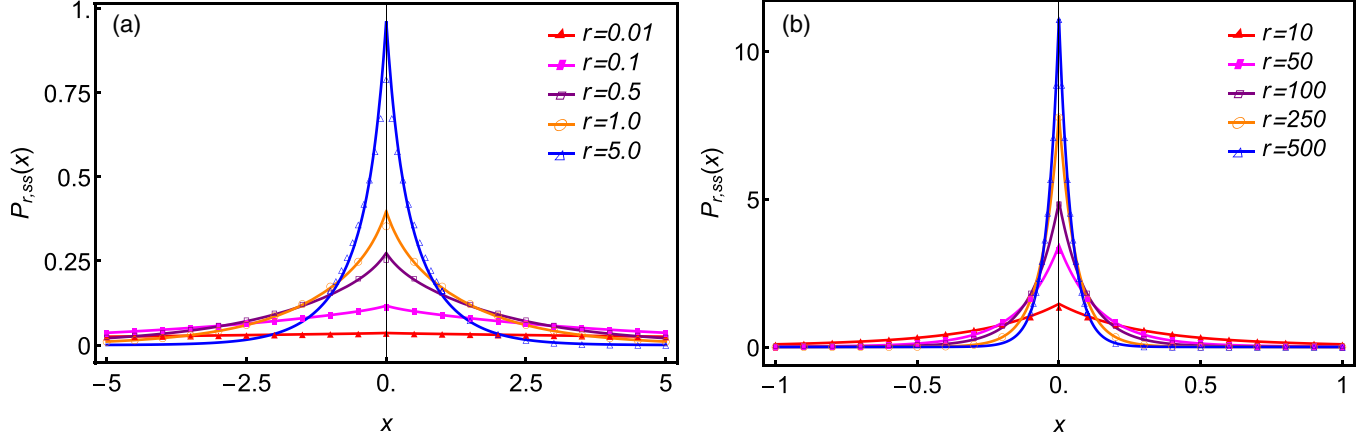
FIG. 1. Plot of the probability distribution function of displacement at the steady state [given in Eq. (12)] for two different regimes of Poisson rates: (a) $r < \mu$, where $\mu = 10$, and (b) $r > \mu$, where $\mu = 5.0$. Here we have taken $D_A = D_T = 1.0$. The curves with point symbols are the approximate analytical results given in Eqs. (14) and (16), and these equations are used for comparison in panels (a) and (b), respectively.

For short-time limits, i.e., for $t \ll 1/r$, the MSD is $\langle x^2(t) \rangle \approx 2(D_A + D_T)t$, implying a short-time diffusive regime, and it is the same as the reset-free case. However, in long-time limits ($t \gg 1/r$), the MSD approaches a constant value, viz., $\langle x^2(t) \rangle \approx \frac{2(D_A + D_T)}{r}$, which indicates the convergence of density to a stationary distribution.

Here we analyze the distribution for the $t \to \infty$ limit. In this case, the first and third terms on the RHS of Eq. (10) can be neglected, and so the distribution becomes

$$P_{r,ss}(x) = \frac{r}{D_T}\left[\left(\frac{\alpha_3(r) - \alpha_1(r)}{\alpha_2(r) - \alpha_1(r)}\right)\frac{e^{-\sqrt{\alpha_1(r)}|x|}}{2\sqrt{\alpha_1(r)}} + \left(\frac{\alpha_2(r) - \alpha_3(r)}{\alpha_2(r) - \alpha_1(r)}\right)\frac{e^{-\sqrt{\alpha_2(r)}|x|}}{2\sqrt{\alpha_2(r)}}\right]. \tag{12}$$

Clearly, Eq. (12) corresponds to the steady-state distribution which is expressed as the sum of two exponential functions. To understand its leading behavior, we consider different limiting cases.

A. Different r limits

Let us first consider the limit $\frac{a_0^2 r}{D_T}(= \frac{D_A}{D_T}\frac{r}{\mu}) \ll 1$. So using the approximation $\sqrt{[\frac{D_A}{D_T} + 1 + \frac{a_0^2 r}{D_T}]^2 - \frac{4a_0^2 r}{D_T}} \approx \frac{D_A}{D_T} + 1 - \frac{2a_0^2 r}{D_A + D_T}$, the parameters can be expressed as $\alpha_1 \approx \frac{r}{[D_A + D_T]}$, $\alpha_2 \approx \frac{1}{a_0^2}(\frac{D_A}{D_T} + 1)$, which leads Eq. (12) to

$$P_{r,ss}(x) \approx \frac{1}{2a_0}\left(1 - \frac{\left(\frac{a_0^2 r}{D_T}\right)\left(\frac{D_A}{D_T}\right)}{\left(\frac{D_A}{D_T} + 1\right)^2}\right)\sqrt{\frac{a_0^2 r}{D_A + D_T}}e^{-\sqrt{\frac{a_0^2 r}{D_A + D_T}}\frac{|x|}{a_0}}$$

$$+ \frac{1}{2a_0}\frac{\left(\frac{a_0^2 r}{D_T}\right)\left(\frac{D_A}{D_T}\right)}{\left(\frac{D_A}{D_T} + 1\right)^2}\sqrt{\left(\frac{D_A}{D_T} + 1\right)}e^{-\sqrt{\frac{D_A}{D_T} + 1}\frac{|x|}{a_0}}. \tag{13}$$

In the above equation, the second term on the RHS captures the behavior near $x = 0$, and it can be neglected for $\frac{a_0^2 r}{D_T} \ll 1$. Here, the first term dominates, and thus the distribution can be approximated as

$$P_{r,ss}(x) \approx \frac{1}{2}\sqrt{\frac{r}{D_A + D_T}}e^{-\sqrt{\frac{r}{D_A + D_T}}|x|}. \tag{14}$$

Such limiting case can be obtained if $r \ll \mu$ and D_A/D_T is finite. At $r \to 0$, the distribution almost flattens as exemplified

in Fig. 1(a) for $r = 0.01$. Within this regime, if $r > \mu$, then $D_T \gg D_A$, and thus, $P_{r,ss}(x) \approx \frac{1}{2}\sqrt{\frac{r}{D_T}}e^{-\sqrt{\frac{r}{D_T}}|x|}$.

Now we consider the limit $\frac{a_0^2 r}{D_T}(= \frac{D_A}{D_T}\frac{r}{\mu}) \gg 1$. In this limit, $\sqrt{[\frac{D_A}{D_T} + 1 + \frac{a_0^2 r}{D_T}]^2 - \frac{4a_0^2 r}{D_T}} \approx \frac{D_A}{D_T} + \frac{a_0^2 r}{D_T} - \frac{2a_0^2 r}{D_A + a_0^2 r}$, $\alpha_1 \approx \frac{1}{a_0^2}\frac{a_0^2 r}{D_A + a_0^2 r} \approx \frac{1}{a_0^2}\frac{1}{[1 + \frac{\mu}{r}]}$, and $\alpha_2 \approx \frac{1}{a_0^2}\frac{D_A}{D_T}[1 + \frac{r}{\mu}]$. So the steady-state distribution (12) becomes

$$P_{r,ss}(x) \approx \frac{1}{2a_0}\frac{1 + \frac{\mu}{r}}{(2 + \frac{r}{\mu} + \frac{\mu}{r})\sqrt{1 + \frac{\mu}{r}}}e^{-\sqrt{\frac{1}{[1 + \frac{\mu}{r}]}}\frac{|x|}{a_0}}$$

$$+ \frac{1}{2a_0}\frac{1 + \frac{r}{\mu}}{(2 + \frac{r}{\mu} + \frac{\mu}{r})}\sqrt{\frac{D_A}{D_T}\left(1 + \frac{r}{\mu}\right)}e^{-\sqrt{\frac{D_A}{D_T}(1 + \frac{r}{\mu})}\frac{|x|}{a_0}}. \tag{15}$$

Here we can consider a limit, $r \gg \mu$, and D_T/D_A is finite. For such case,

$$P_{r,ss}(x) \approx \frac{1}{2a_0}\frac{\mu}{r}e^{-\frac{|x|}{a_0}} + \frac{1}{2}\left(1 - \frac{\mu}{r}\right)\sqrt{\frac{r}{D_T}}e^{-\sqrt{\frac{r}{D_T}}|x|}. \tag{16}$$

In the above equation, the first term on the RHS can be ignored, and so the distribution is given by $P_{r,ss}(x) \approx \frac{1}{2}\sqrt{\frac{r}{D_T}}e^{-\sqrt{\frac{r}{D_T}}|x|}$. For large values of r, the distribution is mostly peaked around $x_0 = 0$, in accordance with Fig. 1(b), as the particle is brought back frequently to the origin and thus it is mostly found there. For the case where $r < \mu$ and $D_A \gg D_T$, the first term on the RHS in Eq. (15) mostly
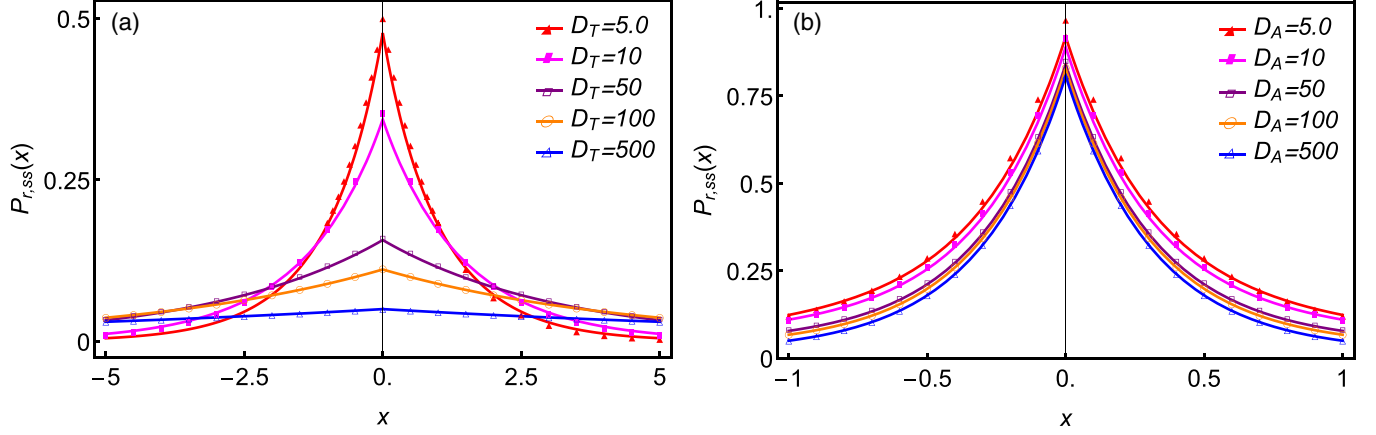
FIG. 2. Plot of the probability distribution functions [Eq. (12)] as a function of displacements for different values of D_A/D_T. In panel (a) $D_T > D_A$, where we have taken $D_A = 1.0$. In panel (b) $D_A > D_T$, where $D_T = 1.0$. Other parameters are $r = \mu = 5.0$. Approximate results of the PDF given in Eqs. (17) and (18) represented by the lines with point symbols are in good agreement with the exact one (solid lines) as shown in panels (a) and (b), respectively.

contributes to the tail behavior, and around $x = 0$ the second term gives a delta function, viz., $\delta(x)/(1 + \frac{\mu}{r})$.

B. Different limits of (D_A/D_T)

We first consider the limit $\frac{D_A}{D_T} \ll 1$, where $\sqrt{[\frac{D_A}{D_T} + 1 + \frac{a_0^2 r}{D_T}]^2 - \frac{4 a_0^2 r}{D_T}} \approx |1 - \frac{a_0^2 r}{D_T}|$. For $\frac{a_0^2 r}{D_T} > 1$, $\alpha_1(r) \approx 1/a_0^2$, and $\alpha_2(r) \approx \frac{r}{D_T}$. In the other limit, $\frac{a_0^2 r}{D_T} < 1$, $\alpha_1(r)$ and $\alpha_2(r)$ just exchange their values. Therefore, for both cases, Eq. (12) approximates to

$$P_{r,ss}(x) \approx \frac{1}{2}\sqrt{\frac{r}{D_T}}\, e^{-\sqrt{\frac{r}{D_T}}|x|}. \tag{17}$$

Here, the thermal contribution prevails over the active one, and as expected, we recover the well-known result for the normal diffusion with resetting. This is consistent with Fig. 2(a).

Now we take the limit $\frac{D_A}{D_T} \gg 1$. So one can do the following approximations: $\sqrt{[\frac{D_A}{D_T} + 1 + \frac{a_0^2 r}{D_T}]^2 - \frac{4 a_0^2 r}{D_T}} \approx \frac{D_A}{D_T} + \frac{a_0^2 r}{D_T} - \frac{2 a_0^2 r}{D_A + a_0^2 r}$, $\alpha_2(r) \approx \frac{1}{a_0^2}[\frac{D_A}{D_T} + \frac{a_0^2 r}{D_T}]$, $\alpha_1(r) \approx \frac{r}{D_A + a_0^2 r} = \frac{1}{a_0^2}\frac{1}{1 + \frac{\mu}{r}}$. Therefore, using Eq. (12) one has

$$P_{r,ss}(x) \approx \frac{1}{2}\left(\frac{D_A}{D_A + a_0^2 r}\right)\sqrt{\frac{r}{D_A + a_0^2 r}}\, e^{-\sqrt{\frac{r}{D_A + a_0^2 r}}|x|}$$
$$+ \frac{1}{2 a_0}\left(\frac{a_0^2 r}{D_A + a_0^2 r}\right)\sqrt{\frac{D_A}{D_T} + \frac{a_0^2 r}{D_T}}\, e^{-\sqrt{\frac{D_A}{D_T} + \frac{a_0^2 r}{D_T}}\frac{|x|}{a_0}}. \tag{18}$$

The first term on the RHS dictates large-x behavior whereas the second one only contributes to the distribution at $x = 0$. Such features can be easily seen in Fig. 2(b). For $\frac{a_0^2 r}{D_A} \ll 1$ or $\frac{r}{\mu} \ll 1$, the PDF can be approximated as $P_{r,ss}(x) \approx \frac{1}{2}\sqrt{\frac{r}{D_A}}e^{-\sqrt{\frac{r}{D_A}}|x|}$, which is of similar form as Eq. (17) with the only difference being that the thermal diffusivity is now replaced by the active one. At $\frac{r}{\mu} \gg 1$, the second term on the RHS of Eq. (18) is dominant over the first one, and thereby

the PDF can be given as $P_{r,ss}(x) \approx \frac{1}{2}\sqrt{\frac{r}{D_T}}\, e^{-\sqrt{\frac{r}{D_T}}|x|} \approx \delta(x)$. Now we consider a situation where only the Poisson noise is present in the system. Therefore, taking $D_T \to 0$ in Eq. (18) the second term turns to a delta function, and so Eq. (18) can be recast as

$$P_{r,ss}(x) \approx \frac{1}{2 a_0}\left(\frac{1}{1 + \frac{r}{\mu}}\right)\sqrt{\frac{1}{1 + \frac{\mu}{r}}}\, e^{-\sqrt{\frac{1}{1+\frac{\mu}{r}}}\frac{|x|}{a_0}} + \left(\frac{1}{1 + \frac{\mu}{r}}\right)\delta(x). \tag{19}$$

III. RELAXATION TO NONEQUILIBRIUM STEADY STATE

Here we analyze how the distribution relaxes to the stationary one at long times. For this purpose, we approximate the distribution after doing the inverse Fourier transform of Eq. (5) as discussed in Appendix C. Two limiting cases for the distribution given in Eq. (C3) are discussed in the following sections.

A. $1 > r \gg \mu$ and $D_T \gg D_A$

The integration over ϕ in Eq. (C3) can be done using the Laplace method, according to which, most nonzero contributions should arise near $\phi = 0$ for the large value of t. In this limit, $I_1(2\mu t'\phi) \approx \mu t'\phi \to 0$ at $\phi = 0$. For $D_T \gg D_A$ and $1 \gg \mu$, the second term on the RHS is negligible compared to the first one. Therefore, $P_r(x, t)$ can be asymptotically given as

$$P_r(x, t) \approx r \int_0^t dt'\, e^{-rt'-\mu t'} \frac{e^{-\frac{x^2}{4 D_T t'}}}{\sqrt{4\pi D_T t'}}.$$

Taking $t' = \omega t$, the above equation can be recast as

$$P_r(x, t) \approx \frac{r t^{1/2}}{\sqrt{4\pi D_T}}\int_0^1 \frac{d\omega}{\sqrt{\omega}}\, e^{-t\Omega_1(v, \omega)}, \tag{20}$$

where the large deviation function (LDF) is $\Omega_1(v, \omega) = r\omega + \mu\omega + \frac{v^2}{4 D_T \omega} \approx r\omega + \frac{v^2}{4 D_T \omega}$ for $r \gg \mu$, and $v = x/t$. For large value of t, the integration over ω can be performed using the saddle-point method. Most contributions to the integration
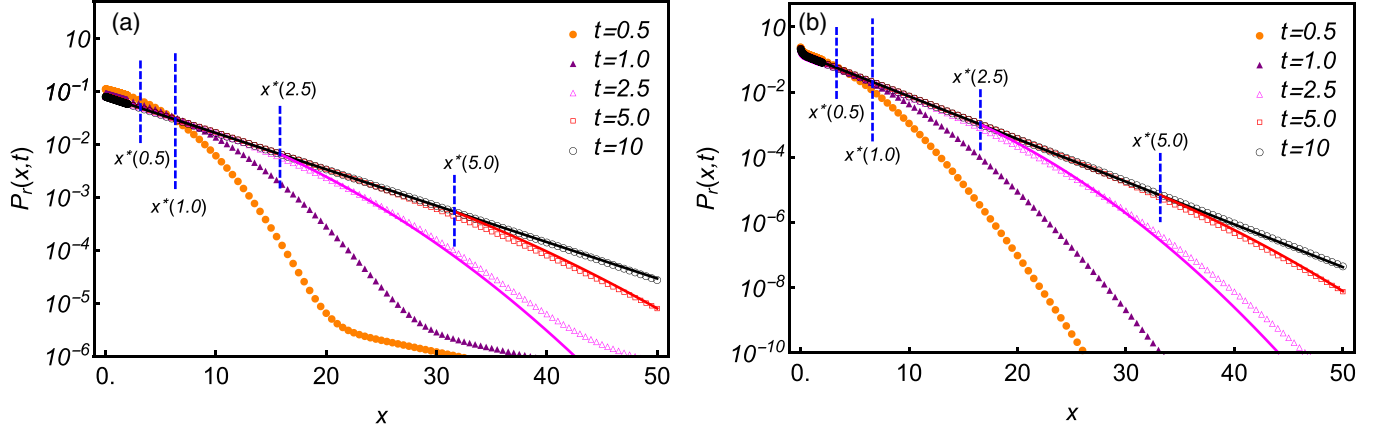
FIG. 3. Comparative plots of analytical results of the complete probability distribution function (PDF) with the numerical one in logarithmic scale as a function of displacements at different times. The dotted curves are plotted using the data obtained from the numerical inverse Fourier transform of Eq. (8). The position $x^*(t)$ which distinguishes two regimes is marked by blue dashed vertical lines for different times. In panels (a) and (b) the plots are for two limiting cases: (a) $\mu \ll 1$, $D_T \gg D_A$ and (b) $\mu \gg r$, D_A/D_T is finite. The values of parameters used for computations are given by (a) $D_T = 20$, $D_A = 0.1$, $\mu = 0.001$, $r = 0.5$ and (b) $D_T = 1.0$, $D_A = 10$, $\mu = 40$, $r = 1.0$. The solid lines corresponds to analytical results given in Eqs. (22) and (27) for two respective cases. The black solid (upper) line is for $x(t) < x^*(t)$ whereas other solid curves (magenta, red) represent the PDFs for large values of t (here we have taken $t = 2.5, 5.0, 10$) in the region $x(t) > x^*(t)$.

come where $\Omega_1'(v, \omega^*) = 0$, which means $\omega^* = \frac{|v|}{2\sqrt{D_T r}}$. One can distinguish two distinct regimes across $\omega^* = 1$ as illustrated in Ref. [38]. The minimum of $\Omega_1(v, \omega)$ occurs (i) at ω^* in the region $\omega \in [0, 1)$, and (ii) at $\omega^* = 1$ for $\omega^* > 1$. So the distribution can be described by the following LDFs at large t:

$$\Omega_1(v, \omega) = \begin{cases} \sqrt{\frac{r}{D_T}}|v|, & \text{for } |v| < v^*, \\ r + \frac{v^2}{4D_T}, & \text{for } |v| > v^*, \end{cases} \quad (21)$$

where $v^* = 2\sqrt{D_T r}$, or equivalently, one can define an associated length scale x^* as $x^*(t) = 2\sqrt{D_T r}\, t$. So, in the spatial region $|x| < x^*$, the density relaxes to a steady state, but it is still in the transient regime for $|x| > x^*$. This result is equivalent to one in the normal case, as has been found in Sec. II B. Doing the integration in Eq. (20) and keeping all the terms carefully, we find the pre-exponential factor to be $\frac{r\omega^*}{|v|}$. Therefore, the complete PDF in the entire space can be expressed as

$$P_r(x, t) = \Theta(x^* - |x|)\frac{1}{2}\sqrt{\frac{r}{D_T}}\, e^{-\sqrt{\frac{r}{D_T}}|x|}$$
$$+ \Theta(|x| - x^*)\frac{rt}{|x|}\, e^{-rt - \frac{x^2}{4D_T t}}, \quad (22)$$

where $\Theta(z)$ is the Heaviside step function. The analytical result (22) agrees well with the numerical one shown in Fig. 3(a).

B. $\mu \gg r \geqslant 1$ and D_A/D_T is finite

For large values of t and μ, the first term on the RHS of Eq. (C3) is negligible compared to the second one. Applying the asymptotic form of $I_1(z)$ as mentioned in Appendix C, the

second term can be approximated as

$$P_r(x, t) \approx 2r \int_0^t (\mu t')dt' \int_0^\infty d\phi\, e^{-rt'}\, \frac{e^{-\mu t'(\phi-1)^2}}{\sqrt{4\pi \mu t' \phi}}$$
$$\times \frac{e^{-\frac{x^2}{4t'(D_T + D_A\phi^2)}}}{\sqrt{4\pi t'(D_T + D_A\phi^2)}}. \quad (23)$$

Now using the saddle-point approximation, the integration over ϕ can be done as most contributions come from the saddle point at $\phi = 1$. Equation (23) approximates to

$$P_r(x, t) \approx \frac{rt^{1/2}}{\sqrt{4\pi(D_A + D_T)}} \int_0^t dt'\, \frac{e^{-\frac{x^2}{4(D_A + D_T)t'}}}{\sqrt{t'}}. \quad (24)$$

For large t, taking $t' = \omega t$, one obtains

$$P_r(x, t) \approx \frac{rt^{1/2}}{\sqrt{4\pi(D_A + D_T)}} \int_0^1 \frac{d\omega}{\sqrt{\omega}}\, e^{-t\Omega_2(v, \omega)}, \quad (25)$$

where the LDF is given by $\Omega_2(v, \omega) = r\omega + \frac{v^2}{4(D_A + D_T)\omega}$, which implies $\omega^* = \frac{|v|}{2\sqrt{(D_A + D_T)r}}$. Like the previous case, we can identify two regimes as follows:

$$\Omega_2(v, \omega) = \begin{cases} \sqrt{\frac{r}{D_A + D_T}}|v|, & \text{for } |v| < v^*, \\ r + \frac{v^2}{4(D_A + D_T)}, & \text{for } |v| > v^*, \end{cases} \quad (26)$$

where $v^* = 2\sqrt{(D_A + D_T)r}$, or $x^* = 2\sqrt{(D_A + D_T)r}\, t$. So putting all terms together, we can write the PDF as

$$P_r(x, t) = \Theta(x^* - |x|)\frac{1}{2}\sqrt{\frac{r}{D_A + D_T}}\, e^{-\sqrt{\frac{r}{D_A + D_T}}|x|}$$
$$+ \Theta(|x| - x^*)\frac{rt}{|x|}\, e^{-rt - \frac{x^2}{4(D_A + D_T)t}}. \quad (27)$$

In Fig. 3(b), Eq. (27) is compared with the PDF computed numerically using Eq. (8), and they are in a good agreement for $t > 1$. The position x^* dictates the partition between two

domains, $|x| < x^*$ and $|x| > x^*$, and it moves linearly with time t. As time progresses, the first domain merges to the second one, and thus the steady state is established in the entire space. For $D_A \gg D_T$, the distribution at the steady state can be computed using Eq. (27), as $P_{r,ss}(x) \approx \frac{1}{2}\sqrt{\frac{r}{D_A}}e^{-\sqrt{\frac{r}{D_A}}|x|}$, and the speed at which the first domain grows mostly depends on D_A, or more specifically, the system reaches quickly to the steady state as the strength of nonthermal fluctuations increases.

IV. FIRST-ARRIVAL PROBLEM

Here we address the first-arrival problem for a particle diffusing in the presence of a target at position $x = x_s$. The particle was initially at position $x = x_0$ ($\neq x_S$), and it is under the Poissonian resetting mechanism which resets the particle to position x_0 at random times with a fixed rate r. The probability of finding the particle diminishes when it encounters the target, which can be thought of as a trap and is modeled here by a delta-function sink of strength κ [60–64]. The particle disappears on arriving at the sink if the value of κ goes to infinity. The time it takes to reach the sink is a random variable, and for the reset-free case in a semi-infinite region, the average time is infinite. But in the presence of resetting, the time is usually finite and takes a minimum value at some resetting rate r^*. Clearly this leads to a more efficient search strategy. For finite values of κ, the particle is not completely absorbed on its first arrival at $x = x_s$ (partial absorption), and so it visits the sink multiple times throughout its journey before it gets annihilated at the sink. As mentioned in Sec. I, there are several cellular processes where reactants cannot recognize the target site at all times. For instance, the transcription is initiated when the protein called the transcription factor (TF) binds to a promoter site on the DNA backbone, but depending on the folding state of chromatin, the site becomes "visible" or "hidden" to the protein. Only in the visible state, the binding happens [65,66]. Such reactions can be conceived as a form of the partial absorption in the presence of a delta sink with finite κ.

We are dealing here with the process which is Markovian in nature, i.e., the absence of any memory into the dynamics. For such processes, one can find the first-arrival time density using the Green's function method as detailed in [60,63]. Without any resetting, the first-arrival time density (FATD) is denoted as $f_{T_0}(t)$, and its Laplace transform is given by $\tilde{f}_{T_0}(s) = \int_0^\infty dt\, e^{-st} f_{T_0}(t)$. So in the presence of a sink of strength κ, the FATD in the Laplace domain can be expressed as [63,67]

$$\tilde{f}_{T_0}(s) = \frac{\kappa \tilde{P}_0(x_s, s|x_0)}{1 + \kappa \tilde{P}_0(x_s, s|x_s)}, \tag{28}$$

where $P_0(x, t|x_0)$ is the free propagator, given by $P_0(x, t|x_0) = \int \frac{dp}{2\pi} e^{-ip(x-x_0)} e^{-(D_T p^2 t + D_A t \frac{p^2}{1+p^2})}$ [see Eq. (2)], and its Laplace transform is [see Eq. (12)]

$$\tilde{P}_0(x, s|x_0) = \frac{P_{r,ss}(x)|_{r=s}}{r}$$
$$= \int_0^\infty dt\, e^{-st} P_0(x, t|x_0)$$

$$= \left(\frac{\alpha_3(s) - \alpha_1(s)}{\alpha_2(s) - \alpha_1(s)}\right)\frac{e^{-\sqrt{\alpha_1(s)}|x-x_0|}}{2D_T\sqrt{\alpha_1(s)}}$$
$$+ \left(\frac{\alpha_2(s) - \alpha_3(s)}{\alpha_2(s) - \alpha_1(s)}\right)\frac{e^{-\sqrt{\alpha_2(s)}|x-x_0|}}{2D_T\sqrt{\alpha_2(s)}}. \tag{29}$$

Let us now invoke the resetting mechanism to the given problem as described earlier. With resetting, the FATD in the Laplace domain can be expressed in terms of $\tilde{f}_{T_0}(s)$ given in Eq. (28), as [68]

$$\tilde{f}_{T_r}(s) = \frac{\tilde{f}_{T_0}(s+r)}{\frac{s}{s+r} + \frac{r}{s+r}\tilde{f}_{T_0}(s+r)}. \tag{30}$$

An important quantity for a search process is the mean first-arrival time (MFAT) which is basically the first moment of FATD. So it can be easily calculated using the following expression:

$$\langle \mathbb{T}_r \rangle = -\frac{\partial \tilde{f}_{T_r}(s)}{\partial s}\bigg|_{s=0} = \frac{1}{r}\frac{1}{\tilde{f}_{T_0}(r)} - \frac{1}{r}$$
$$= \frac{1}{r}\frac{1 + \kappa \tilde{P}_0(x_s, r|x_s)}{\kappa \tilde{P}_0(x_s, r|x_0)} - \frac{1}{r}. \tag{31}$$

Employing the analysis done in Sec. II A (for the limiting case $\frac{a_0^2 r}{D_T} \ll 1$), one can obtain, for small values of r,

$$\tilde{P}_0(x_s, r|x_0) \approx \frac{1}{2r}\sqrt{\frac{r}{D_T + D_A}}e^{-\sqrt{\frac{r}{D_T+D_A}}|x_s-x_0|}.$$

Using the above, the MFAT can be approximated as

$$\langle \mathbb{T}_r \rangle \approx \frac{1}{r}\frac{2r\sqrt{\frac{D_T+D_A}{r}} + \kappa}{\kappa\, e^{-\sqrt{\frac{r}{D_T+D_A}}|x_s-x_0|}} - \frac{1}{r} \approx \frac{1}{r}\left(e^{\sqrt{\frac{r}{D_T+D_A}}|x_s-x_0|} - 1\right)$$
$$+ \frac{2}{\kappa}\sqrt{\frac{D_T+D_A}{r}}e^{\sqrt{\frac{r}{D_T+D_A}}|x_s-x_0|}. \tag{32}$$

At $r \to 0$, $\langle \mathbb{T}_r \rangle \approx \sqrt{\frac{1}{r(D_A+D_T)}}|x_s - x_0| + \frac{2}{\kappa}\sqrt{\frac{D_T+D_A}{r}} + \frac{2}{\kappa}|x_s - x_0|$. In the case of complete absorption ($\kappa \to \infty$), the MFAT can be written as $\langle \mathbb{T}_r \rangle \approx \sqrt{\frac{1}{r(D_A+D_T)}}|x_s - x_0|$. As expected, for no resetting case, $\langle \mathbb{T}_r \rangle$ diverges as $r^{-1/2}$ as $r \to 0$. For the case where only the thermal noise acts on the particle, i.e., $D_A \to 0$, the MFAT given in Eq. (32) transforms to

$$\langle \mathbb{T}_r \rangle \approx \frac{1}{r}\left(e^{\sqrt{\frac{r}{D_T}}|x_s-x_0|} - 1\right) + \frac{2}{\kappa}\sqrt{\frac{D_T}{r}}e^{\sqrt{\frac{r}{D_T}}|x_s-x_0|}, \tag{33}$$

which is equivalent to the one given in Ref. [56]. For $D_A \gg D_T$ and small values of r,

$$\langle \mathbb{T}_r \rangle \approx \frac{1}{r}\left(e^{\sqrt{\frac{r}{D_A}}|x_s-x_0|} - 1\right) + \frac{2}{\kappa}\sqrt{\frac{D_A}{r}}e^{\sqrt{\frac{r}{D_A}}|x_s-x_0|}. \tag{34}$$

For extremely large values of r and finite values of D_A and D_T, we can have $\tilde{P}_0(x_s, r|x_0) \approx \frac{1}{2r}\sqrt{\frac{r}{D_T}}e^{-\sqrt{\frac{r}{D_T}}|x_s-x_0|}$, and therefore, the MFAT can be described by Eq. (33).

Figure 4(a) demonstrates results for the MFAT as a function of resetting rate r for different values of κ. In the limits, $r \to 0$ and $r \to \infty$, $\langle \mathbb{T}_r \rangle$ blows up to infinity as can be understood from Fig. 4. This can be explained as follows:
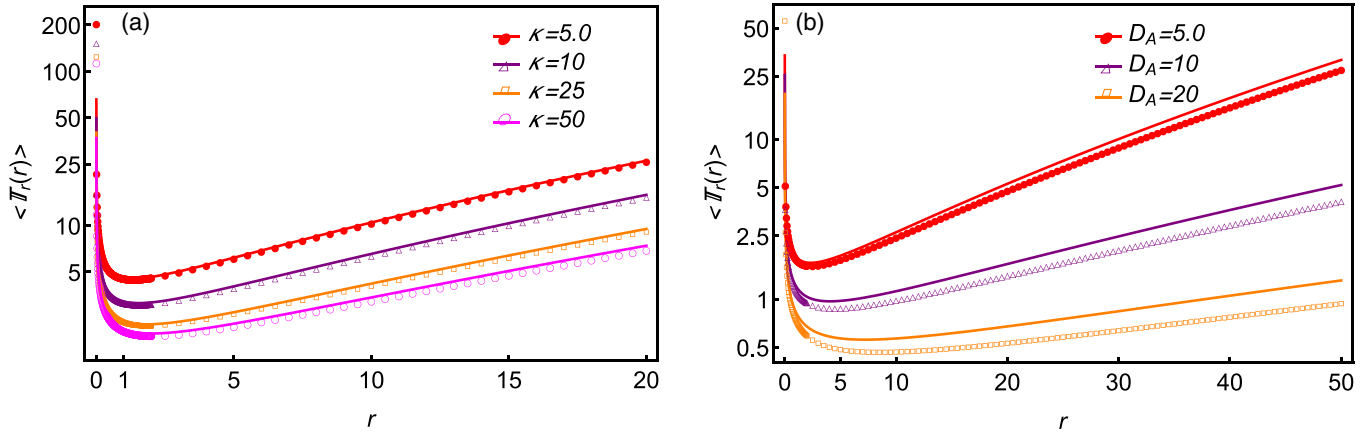
FIG. 4. Logarithmic plot of first-passage times versus resetting rate r: (a) for different values of sink strength κ taking $D_A = 5.0, D_T = 1.0$ and (b) for different D_A values keeping the thermal diffusivity constant at $D_T = 1.0$ in the case of complete absorption. The solid curves are drawn by solving Eq. (31) numerically taking $\mu = 5000$ and assuming that the distance between the sink and the source is fixed at $|x_s - x_0| = 2.50$. The dotted curves correspond to Eq. (32) which is a quite approximate result for the limit $\frac{D_A}{D_T} \frac{r}{\mu} \ll 1$. In panel (a) the solid curves agree well with the analytical results for the given range of Poisson rate r, whereas the dotted lines are good fits only for small values of r if D_A is large, as shown in panel (b).

For $r \to 0$, some trajectories can never cross the sink due to almost no resetting, and this leads to infinite MFAT. On the other hand, if $r \to \infty$, the particle is reset so frequently that it always remains near the initial position and so it never reach the sink. In between these extreme limits, $\langle \mathbb{T}_r \rangle$ varies nonmonotonically, namely, the MFAT decreases with r until it reaches to a minimum. So there exists an optimal resetting rate r^* for which one has $\frac{d}{dr} \langle \mathbb{T}_r \rangle|_{r=r^*} = 0$. One needs to solve the previous transcendental equation which, unfortunately, cannot be done analytically. For different values of κ and D_A, the optimal rates r^* have been computed numerically and shown in Fig. 5. From Fig. 5(a), one can notice that r^* increases with κ, but it reaches to a fixed value in the large-κ limit which basically corresponds to the complete absorption. For the case of the partial absorption (i.e., κ is small) the particle can easily

jump over the sink without getting absorbed, and thus it can avail the entire space. This suggests that the particle can reach the target from both sides in one-dimensional space. However, for large κ, the absorption happens mostly from one side, and thus the process is required to reset more frequently in order to achieve an optimal rate. Figure 4(a) shows the plot of the MFAT as a function of sink strength. Notice that the MFAT is lower for large values of κ as the chances of survival for the particle decrease if the sink has a higher strength.

In Fig. 4(b), it has been shown that the MFAT, as usual, is a nonmonotonic function of r for any value of D_A. But for a bath with a fixed thermal diffusivity, the MFAT decreases if the strength (or diffusivity) of athermal noise is large. This is easy to understand because these extra fluctuations push the particle away from its initial position and thus help to
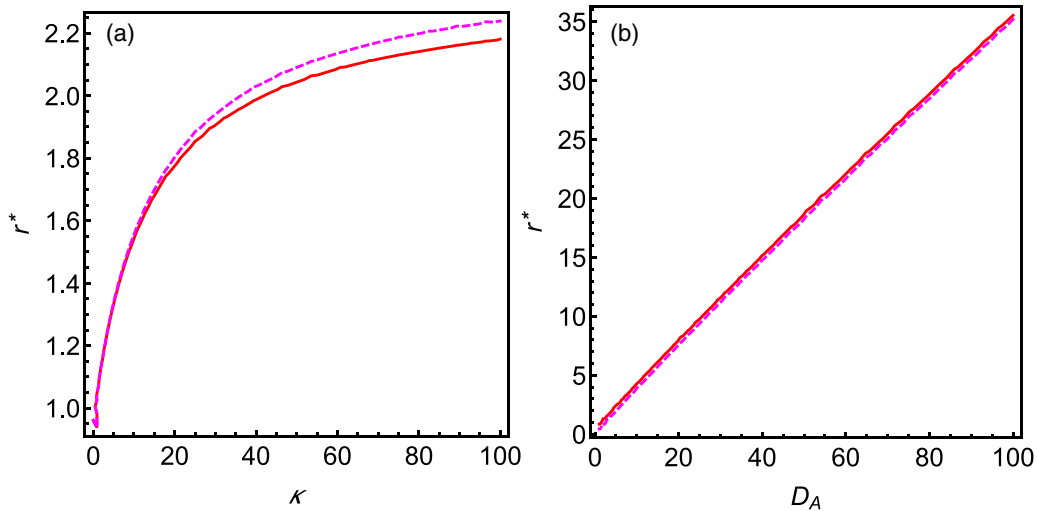

FIG. 5. (a) Plot of optimal rate r^* as a function of the sink strength κ. The other parameters are $D_A = 5.0, D_T = 1.0$. (b) The optimal rate r^* for complete absorption is plotted against D_A considering D_T constant at $D_T = 1.0$. The curves are obtained by solving the equation $\frac{d}{dr} \langle \mathbb{T}_r \rangle|_{r=r^*} = 0$. Solid lines correspond to the exact results computed with the aid of Eqs. (31) and (29), and approximate result given in Eq. (32) is used to draw the dashed lines. For both panels (a) and (b), the other parameters taken for numerical calculation are given here: $|x_s - x_0| = 2.50, a_0 = 0.02236$.

locate the target quickly. However, for such acceleration of the process, one has to bear the cost of its opposing mechanism, i.e., Poissonian resetting. This means that the density which is transferred far away from the sink in the opposite direction due to robust diffusive mechanism needs to be brought back to the initial position repeatedly so that the particle can restart its journey toward the sink. So the optimal rate r^* is an increasing function of D_A, as pictorially depicted in Fig. 5(b).

V. CONCLUSION

We have investigated the effect of Poissonian resetting on a diffusing particle in a nonthermal bath. In contrast to the thermal case, the steady-state distribution is described by two exponential functions, one for the central region and another depicting the tail behavior. At transient periods, we have identified two distinct regimes, and have shown how the transient regime gradually relaxes to the stationary one over time, and the speed at which the relaxation occurs depends on the strengths of the noises. In the presence of a target, it has been found that the existence of additional noise aids the particle to find the target easily, although in order to get an optimal search rate, the particle is required to reset more frequently.

Searching under a resetting protocol appears to be an effective strategy for a plethora of systems [38]. In particular, for biological systems where a reaction often starts after a reactant finds a target, the invocation of the resetting mechanism to a reaction becomes very much relevant. Our study essentially focuses on similar aspects where the first arrival of a particle to the sink denotes the beginning of a reaction and its reversibility is captured via the sink strength. Therefore, our findings bring out a generic perspective of any Markovian biophysical processes under resetting. However, for a non-Markovian process (e.g., see Refs. [12,13,24]), one requires a different formalism which can be investigated in future.

ACKNOWLEDGMENTS

APPENDIX A: DERIVATION OF EQUATION (2)

Poisson white noise (PWN) can be realized as sum of pulses $g(t_i)$ with amplitude a_i at different times t_i as

$$\xi_A(t) = \sum_i a_i \, g(t - t_i).$$

The number of delta pulses n over a time period $[0, t]$ are drawn from the Poisson distribution with a Poisson rate μ, viz.,

$$\mathcal{P}(n, t; \mu) = \sum_{n=0}^{n=\infty} \frac{(\mu t)^n}{n!} e^{-\mu t}. \tag{A1}$$

For such noise, the characteristic functional can be expressed as [69]

$$\langle e^{i \int_0^t dt_1 \, p(t_1)\xi_A(t_1)} \rangle_{\xi_A(t_1)} = e^{-\mu \int_0^t dt_1 \{1 - W[\int_0^{t_1} dt_2 \, p(t_2)g(t_1 - t_2)]\}}, \tag{A2}$$

where $W[\psi] = \int_{-\infty}^{+\infty} da \, P(a)e^{ia\psi}$.

The probability distribution of a is $P(a)$, and if we consider $P(a)$ as the Laplace distribution with scale parameter $a_0 \, (> 0)$, i.e., $P(a) = \frac{1}{2a_0} e^{-\frac{|a|}{a_0}}$, we get $W[\psi] = \frac{1}{2a_0} \int_{-\infty}^{+\infty} da \, e^{-\frac{|a|}{a_0}} e^{ia\psi} = \frac{1}{1+a_0^2\psi^2}$. Using this in Eq. (A2), one obtains

$$\langle e^{i \int_0^t dt_1 \, p(t_1)\xi_A(t_1)} \rangle_{\xi_A(t_1)} = e^{-\mu \int_0^t dt_1 \frac{a_0^2 [\int_0^{t_1} dt_2 \, p(t_2)g(t_1 - t_2)]^2}{1 + a_0^2 [\int_0^{t_1} dt_2 \, p(t_2)g(t_1 - t_2)]^2}}. \tag{A3}$$

Now taking $g(t) = \delta(t)$, one has $\int_0^{t_1} dt_2 \, p(t_2)g(t_1 - t_2) = p(t_1)$, and so Eq. (A3) becomes

$$\langle e^{i \int_0^t dt_1 \, p(t_1)\xi_A(t_1)} \rangle_{\xi_A(t_1)} = e^{-\mu \int_0^t dt_1 \frac{a_0^2 p(t_1)^2}{1 + a_0^2 p(t_1)^2}}. \tag{A4}$$

For our model, the dynamical equation reads

$$\dot{x}(t) = \eta_T(t) + \xi_A(t), \tag{A5}$$

which means that we can write the Fourier transform of the PDF as

$$\tilde{P}_0(p, t) = \langle e^{ipx} \rangle = \langle e^{ip \int_0^t dt_1 \eta_T(t_1)} \rangle_{\eta_T(t_1)} \langle e^{ip \int_0^t dt_1 \xi_A(t_1)} \rangle_{\xi_A(t_1)}. \tag{A6}$$

For thermal noise, $\langle e^{ip \int_0^t dt_1 \eta_T(t_1)} \rangle_{\eta_T(t_1)} = e^{-D_T p^2 \int_0^t dt_1} = e^{-D_T p^2 t}$, and for noise $\xi_A(t)$, by virtue of Eq. (A4) one has

$$\langle e^{ip \int_0^t dt_1 \xi_A(t_1)} \rangle_{\xi_A(t_1)} = e^{-\mu t \frac{a_0^2 p^2}{1 + a_0^2 p^2}}. \tag{A7}$$

So one can write the Fourier transform as

$$\tilde{P}_0(p, t) = e^{-D_T p^2 t - \mu t \frac{a_0^2 p^2}{1 + a_0^2 p^2}}, \tag{A8}$$

which is the same as Eq. (2) ($D_A = \mu a_0^2$). Note that in Sec. II we get the result solving the Fokker-Planck equation (1) which is equivalent to the Langevin equation (A5). Taking the derivative of the above with respect to time t, one has

$$\frac{\partial}{\partial t} \tilde{P}_0(p, t) = -\left[D_T p^2 + \mu \frac{a_0^2 p^2}{1 + a_0^2 p^2} \right] \tilde{P}_0(p, t)$$

$$= -D_T p^2 \tilde{P}_0(p, t) - \mu a_0^2 p^2 \sum_{n=0}^{\infty} \left(-a_0^2 p^2 \right)^n \tilde{P}_0(p, t). \tag{A9}$$

On doing the inverse Fourier transform, we have

$$\frac{\partial}{\partial t} P_0(x, t) = D_T \frac{\partial^2}{\partial x^2} P_0(x, t) + D_A \frac{\partial^2}{\partial x^2} \sum_{n=0}^{\infty} \left(a_0^2 \right)^n \left(\frac{\partial^2}{\partial x^2} \right)^n$$

$$\times P_0(x, t)$$

$$= D_T \frac{\partial^2}{\partial x^2} P_0(x, t) + D_A \frac{\frac{\partial^2}{\partial x^2}}{1 - a_0^2 \frac{\partial^2}{\partial x^2}} P_0(x, t), \tag{A10}$$

which is the same as Eq. (1).

APPENDIX B: SOLVING EQUATION (5)

To solve Eq. (5), first Eq. (4) is rewritten as

$$\frac{\partial}{\partial t}\tilde{P}_r(p,t) + \left[D_T p^2 + D_A \frac{p^2}{1+a_0^2 p^2} + r\right]\tilde{P}_r(p,t) = r e^{-ipx_0}.$$

Multiplying both sides by the integrating factor,

$$e^{rt+D_T t p^2 + D_A t \frac{p^2}{1+a_0^2 p^2}}\frac{\partial}{\partial t}\tilde{P}_r(p,t) + e^{rt+D_T t p^2 + D_A t \frac{p^2}{1+a_0^2 p^2}}\left[D_T p^2 + D_A \frac{p^2}{1+a_0^2 p^2} + r\right]\tilde{P}_r(p,t) = r e^{rt+D_T t p^2 + D_A t \frac{p^2}{1+a_0^2 p^2}} e^{-ipx_0},$$

which implies

$$\frac{\partial}{\partial t}\left[e^{rt+D_T t p^2 + D_A t \frac{p^2}{1+a_0^2 p^2}}\tilde{P}_r(p,t)\right] = r e^{rt+D_T t p^2 + D_A t \frac{p^2}{1+a_0^2 p^2}} e^{-ipx_0}. \tag{B1}$$

Integrating the above, one can obtain

$$\tilde{P}_r(p,t) - \tilde{P}_r(p,0)e^{-rt-D_T t p^2 - D_A t \frac{p^2}{1+a_0^2 p^2}} = r\int_0^t dt_1 e^{-r(t-t_1)+D_T p^2(t-t_1)+D_A \frac{p^2}{1+a_0^2 p^2}(t-t_1)} e^{-ipx_0}.$$

Taking $x_0 = 0$, and using Eq. (2), $\tilde{P}_0(p,t) = e^{-D_T p^2 t - D_A t \frac{p^2}{1+a_0^2 p^2}}$, one can arrive at Eq. (5).

APPENDIX C: LONG-TIME BEHAVIOR OF EQUATION (10)

Following the procedure described in Ref. [8], we rewrite Eq. (5) as

$$\tilde{P}_r(p,t) = e^{-rt} e^{-D_T p^2 t - D_A t \frac{p^2}{1+a_0^2 p^2}} + r\int_0^t dt' e^{-rt'} e^{-D_T p^2 t' - \mu t'}\sum_{n=0}^{\infty}\frac{(\mu t')^n}{n!}\left(\frac{1}{1+a_0^2 p^2}\right)^n$$

$$= e^{-rt} e^{-D_T p^2 t - D_A t \frac{p^2}{1+a_0^2 p^2}} + r\int_0^t dt' e^{-rt'-D_T p^2 t' - \mu t'} + r\int_0^t dt' e^{-rt'-D_T p^2 t' - \mu t'}\sum_{n=1}^{\infty}\frac{(\mu t')^n}{n!}\left(\frac{1}{1+a_0^2 p^2}\right)^n. \tag{C1}$$

For large t, the first term on the RHS diminishes to zero. So we only consider the other terms and rewrite Eq. (C1) as

$$\tilde{P}_r(p,t) \approx r\int_0^t dt' e^{-rt'-D_T p^2 t' - \mu t'} + r\int_0^t dt' e^{-rt'-D_T p^2 t' - \mu t'}\sum_{n=0}^{\infty}\frac{(\mu t')^{n+1}}{(n+1)!}\left(\frac{1}{1+a_0^2 p^2}\right)^{n+1}$$

$$\approx r\int_0^t dt' e^{-rt'-D_T p^2 t' - \mu t'} + r\int_0^t dt' e^{-rt'-D_T p^2 t' - \mu t'}\sum_{n=0}^{\infty}\frac{(\mu t')^{n+1}}{(n+1)!n!}\left\{\left(-\frac{\partial}{\partial\beta}\right)^n\int_0^{\infty} d\phi\,(2\phi\mu t')e^{-\phi^2\mu t'(\beta+a_0^2 p^2)}\right\}_{\beta=1}. \tag{C2}$$

On performing the inverse Fourier transform of the above and doing the derivative with respect to β at $\beta = 1$, we have

$$P_r(x,t) \approx r\int_0^t dt' e^{-rt'-\mu t'}\frac{e^{-\frac{x^2}{4D_T t'}}}{\sqrt{4\pi D_T t'}} + 2r\int_0^t dt'\int_0^{\infty} d\phi\, e^{-rt'-\mu t'-\phi^2\mu t'}\sum_{n=0}^{\infty}\frac{(\mu t')^{2(n+1)}\phi^{2n+1}}{(n+1)!n!}\frac{e^{-\frac{x^2}{4t(D_T+D_A\phi^2)}}}{\sqrt{4\pi t(D_T+D_A\phi^2)}}$$

$$\approx r\int_0^t dt' e^{-rt'-\mu t'}\frac{e^{-\frac{x^2}{4D_T t'}}}{\sqrt{4\pi D_T t'}} + 2r\int_0^t (\mu t')dt'\int_0^{\infty} d\phi\, e^{-rt'-\mu t'-\mu\phi^2 t'} I_1(2\mu t'\phi)\frac{e^{-\frac{x^2}{4t(D_T+D_A\phi^2)}}}{\sqrt{4\pi t(D_T+D_A\phi^2)}}. \tag{C3}$$

In the second step, the sum over n results in $I_1(z)$, which is the modified Bessel function of the first kind. Two useful limiting values of $I_1(z)$ are $I_1(z) \approx \frac{z}{2}$ for $z \ll 1$, and $I_1(z) \approx \frac{e^z}{\sqrt{2\pi z}}$ as $z \gg 1$.

[1] A. Einstein, Über die von der molekularkinetischen Theorie der Wärme geforderte Bewegung von in ruhenden Flüssigkeiten suspendierten Teilchen, Ann. Phys. **322**(8), 549 (1905).

[2] C. Bechinger, R. Di Leonardo, H. Löwen, C. Reichhardt, G. Volpe, and G. Volpe, Active particles in complex and crowded environments, Rev. Mod. Phys. **88**, 045006 (2016).

[3] L. Caprini, Generalized fluctuation-dissipation relations holding in non-equilibrium dynamics, J. Stat. Mech. (2021) 063202.

[4] T. GrandPre, K. Klymko, K. K. Mandadapu, and D. T. Limmer, Entropy production fluctuations encode collective behavior in active matter, Phys. Rev. E **103**, 012613 (2021).

[5] S. Ramaswamy, Active matter, J. Stat. Mech. (2017) 054002.

[6] E. Fodor and M. C. Marchetti, The statistical physics of active matter: From self-catalytic colloids to living cells, Physica A **504**, 106 (2018).

[7] D. Martin, J. O'Byrne, M. E. Cates, É. Fodor, C. Nardini, J. Tailleur, and F. van Wijland, Statistical mechanics of active Ornstein-Uhlenbeck particles, Phys. Rev. E **103**, 032607 (2021).

[8] K. Goswami and K. L. Sebastian, Diffusion caused by two noises—active and thermal, J. Stat. Mech. (2019) 083501.

[9] K. Goswami, Nonequilibrium dynamics and thermodynamics of some single-particle activity-induced diffusive systems, Ph.D. thesis, Indian Institute of Science, 2020.

[10] S. Chaki and R. Chakrabarti, Entropy production and work fluctuation relations for a single particle in active bath, Physica A **511**, 302 (2018).

[11] N. Samanta and R. Chakrabarti, Chain reconfiguration in active noise, J. Phys. A: Math. Gen. **49**, 195601 (2016).

[12] J. Gladrow, N. Fakhri, F. C. MacKintosh, C. F. Schmidt, and C. P. Broedersz, Broken Detailed Balance of Filament Dynamics in Active Networks, Phys. Rev. Lett. **116**, 248301 (2016).

[13] J. Gladrow, C. P. Broedersz, and C. F. Schmidt, Nonequilibrium dynamics of probe filaments in actin-myosin networks, Phys. Rev. E **96**, 022408 (2017).

[14] S. Chaki and R. Chakrabarti, Effects of active fluctuations on energetics of a colloidal particle: Superdiffusion, dissipation and entropy production, Physica A **530**, 121574 (2019).

[15] K. Goswami, Heat fluctuation of a harmonically trapped particle in an active bath, Phys. Rev. E **99**, 012112 (2019).

[16] K. Goswami, Work fluctuations in a generalized Gaussian active bath, Physica A **566**, 125609 (2021).

[17] K. Goswami, Work fluctuation relations for a dragged Brownian particle in active bath, Physica A **525**, 223 (2019).

[18] T. Toyota, D. A. Head, C. F. Schmidt, and D. Mizuno, Non-Gaussian athermal fluctuations in active gels, Soft Matter **7**, 3234 (2011).

[19] B. Stuhrmann, M. Soarese Silva, M. Depken, F. C. MacKintosh, and G. H. Koenderink, Nonequilibrium fluctuations of a remodeling in vitro cytoskeleton, Phys. Rev. E **86**, 020901(R) (2012).

[20] É. Fodor, M. Guo, N. S. Gov, P. Visco, D. A. Weitz, and F. van Wijland, Activity-driven fluctuations in living cells, Europhys. Lett. **110**, 48005 (2015).

[21] N. Gov, Membrane Undulations Driven by Force Fluctuations of Active Proteins, Phys. Rev. Lett. **93**, 268104 (2004).

[22] E. Ben-Isaac, Y. Park, G. Popescu, F. L. H. Brown, N. S. Gov, and Y. Shokef, Effective Temperature of Red-Blood-Cell Membrane Fluctuations, Phys. Rev. Lett. **106**, 238103 (2011).

[23] M. J. Chacron, B. Lindner, and A. Longtin, Noise Shaping by Interval Correlations Increases Information Transfer, Phys. Rev. Lett. **92**, 080601 (2004).

[24] S. Chaki and R. Chakrabarti, Enhanced diffusion, swelling, and slow reconfiguration of a single chain in non-Gaussian active bath, J. Chem. Phys. **150**, 094902 (2019).

[25] K. Kanazawa, T. Sagawa, and H. Hayakawa, Stochastic Energetics for Non-Gaussian Processes, Phys. Rev. Lett. **108**, 210601 (2012).

[26] K. Kanazawa, T. G. Sano, T. Sagawa, and H. Hayakawa, Minimal Model of Stochastic Athermal Systems: Origin of Non-Gaussian Noise, Phys. Rev. Lett. **114**, 090601 (2015).

[27] W. A. M. Morgado and S. M. D. Queirós, Thermostatistics of small nonlinear systems: Poissonian athermal bath, Phys. Rev. E **93**, 012121 (2016).

[28] E. Fodor, H. Hayakawa, J. Tailleur, and F. van Wijland, Non-Gaussian noise without memory in active matter, Phys. Rev. E **98**, 062610 (2018).

[29] T. Gera and K. L. Sebastian, Solution to the Kramers barrier crossing problem caused by two noises: Thermal noise and Poisson white noise, J. Chem. Phys. **155**, 014902 (2021).

[30] P. Reimann, Brownian motors: Noisy transport far from equilibrium, Phys. Rep. **361**, 57 (2002).

[31] Y. Nishigami, H. Ito, S. Sonobe, and M. Ichikawa, Non-periodic oscillatory deformation of an actomyosin microdroplet encapsulated within a lipid interface, Sci. Rep **6**, 1 (2016).

[32] T. G. Sano, K. Kanazawa, and H. Hayakawa, Granular rotor as a probe for a nonequilibrium bath, Phys. Rev. E **94**, 032910 (2016).

[33] O. G. Berg and P. H. von Hippel, Diffusion-controlled macromolecular interactions, Annu. Rev. Biophys. Biophys. Chem. **14**, 131 (1985).

[34] M. Bauer and R. Metzler, Generalized facilitated diffusion model for DNA-binding proteins with search and recognition states, Biophys. J. **102**, 2321 (2012).

[35] P. C. Blainey, G. Luo, S. C. Kou, W. F. Mangel, G. L. Verdine, B. Bagchi, and X. S. Xie, Nonspecifically bound proteins spin while diffusing along DNA, Nat. Mol. Str. Biol. **16**, 1224 (2009).

[36] M. R. Evans and S. N. Majumdar, Diffusion with Stochastic Resetting, Phys. Rev. Lett. **106**, 160601 (2011).

[37] M. R. Evans, S. N. Majumdar, and K. Mallick, Optimal diffusive search: Nonequilibrium resetting versus equilibrium dynamics, J. Phys. A: Math. Theor. **46**, 185001 (2013).

[38] M. R. Evans, S. N. Majumdar, and G. Schehr, Stochastic resetting and applications, J. Phys. A: Math. Theor. **53**, 193001 (2020).

[39] V. Méndez, A. Masó-Puigdellosas, T. Sandev, and D. Campos, Continuous time random walks under Markovian resetting, Phys. Rev. E **103**, 022103 (2021).

[40] S. N. Majumdar and G. Oshanin, Spectral content of fractional Brownian motion with stochastic reset, J. Phys. A: Math. Theor. **51**, 435001 (2018).

[41] L. Kuśmierz and E. Gudowska-Nowak, Optimal first-arrival times in Lévy flights with resetting, Phys. Rev. E **92**, 052127 (2015).

[42] D. Gupta, Stochastic resetting in underdamped Brownian motion, J. Stat. Mech. (2019) 033212.

[43] P. C. Bressloff, Directed intermittent search with stochastic resetting, J. Phys. A: Math. Theor. **53**, 105001 (2020).

[44] M. Magoni, S. N. Majumdar, and G. Schehr, Ising model with stochastic resetting, Phys. Rev. Res. **2**, 033182 (2020).

[45] U. Basu, A. Kundu, and A. Pal, Symmetric exclusion process under stochastic resetting, Phys. Rev. E **100**, 032136 (2019).

[46] E. Roldán and S. Gupta, Path-integral formalism for stochastic resetting: Exactly solved examples and shortcuts to confinement, Phys. Rev. E **96**, 022130 (2017).

[47] R. K. Singh, R. Metzler, and T. Sandev, Resetting dynamics in a confining potential, J. Phys. A: Math. Theor. **53**, 505003 (2020).

[48] G. Mercado-Vásquez, D. Boyer, S. N. Majumdar, and G. Schehr, Intermittent resetting potentials, J. Stat. Mech. (2020) 113203.

[49] P. C. Bressloff, Switching diffusions and stochastic resetting, J. Phys. A: Math. Theor. **53**, 275003 (2020).

[50] F. Mori, P. Le Doussal, S. N. Majumdar, and G. Schehr, Universal properties of a run-and-tumble particle in arbitrary dimension, Phys. Rev. E **102**, 042133 (2020).

[51] J. Masoliver, Telegraphic processes with stochastic resetting, Phys. Rev. E **99**, 012121 (2019).

[52] I. Santra, U. Basu, and S. Sabhapandit, Run-and-tumble particles in two dimensions under stochastic resetting conditions, J. Stat. Mech. (2020) 113206.

[53] M. R. Evans and S. N. Majumdar, Run and tumble particle under resetting: A renewal approach, J. Phys. A: Math. Theor. **51**, 475003 (2018).

[54] I. Abdoli and A. Sharma, Stochastic resetting of active Brownian particles with Lorentz force, Soft Matter **17**, 1307 (2021).

[55] J. Masoliver and M. Montero, Anomalous diffusion under stochastic resettings: A general approach, Phys. Rev. E **100**, 042103 (2019).

[56] J. Whitehouse, M. R. Evans, and S. N. Majumdar, Effect of partial absorption on diffusion with resetting, Phys. Rev. E **87**, 022118 (2013).

[57] O. Tal-Friedman, A. Pal, A. Sekhon, S. Reuveni, and Y. Roichman, Experimental realization of diffusion with stochastic resetting, J. Phys. Chem. Lett. **11**, 7350 (2020).

[58] A. A. Dubkov, O. V. Rudenko, and S. N. Gurbatov, Probability characteristics of nonlinear dynamical systems driven by δ-pulse noise, Phys. Rev. E **93**, 062125 (2016).

[59] C. Van Den Broeck, On the relation between white shot noise, Gaussian white noise, and the dichotomic Markov process, J. Stat. Phys. **31**, 467 (1983).

[60] A. Szabo, G. Lamm, and G. H. Weiss, Localized partial traps in diffusion processes and random walks, J. Stat. Phys. **34**, 225 (1984).

[61] B. Bagchi, On the theory of barrierless electronic relaxation in solution, J. Chem. Phys. **87**, 5393 (1987).

[62] B. Bagchi and G. R. Flemming, Dynamics of activationless reactions in solution, J. Phys. Chem. **94**, 9 (1990).

[63] K. L. Sebastian, Theory of electronic relaxation in solution: Exact solution for a delta-function sink in a parabolic potential, Phys. Rev. A **46**, R1732(R) (1992).

[64] A. Debnath, R. Chakrabarti, and K. L. Sebastian, Rate processes with dynamical disorder: A direct variational approach, J. Chem. Phys. **124**, 204111 (2006).

[65] B. Munsky, G. Neuert, and A. Van Oudenaarden, Using gene expression noise to understand gene regulation, Science **336**, 183 (2012).

[66] G. Mercado-Vásquez and D. Boyer, First Hitting Times to Intermittent Targets, Phys. Rev. Lett. **123**, 250603 (2019).

[67] D. Janakiraman, Lévy flights in the presence of a point sink of finite strength, Phys. Rev. E **95**, 012154 (2017).

[68] S. Reuveni, Optimal Stochastic Restart Renders Fluctuations in First Passage Times Universal, Phys. Rev. Lett. **116**, 170601 (2016).

[69] R. P. Feynman, A. R. Hibbs, and D. F. Styer, *Quantum Mechanics and Path Integrals* (Dover Publications, 2010).